7 Nanomaterials and Catalysis

Annelise Kopp Alves[1], Felipe Amorim Berutti[2],
and Felipe Antonio Lucca Sánchez[1]

[1] Universidade Federal do Rio Grande do Sul, 90035190, Porto Alegre, Brazil
[2] Universidade Federal do Pampa, 96413170, Bagé, Brazil

Abstract. Catalysts are typical nanomaterials, perhaps the first nanomaterials in wide applications. Catalysis is a nanoscale phenomenon that has been the subject of research and development for many years, but only recently has it become a nanoscale science of materials and chemistry involving more investigations on the molecular level. Nanomaterial-based catalysts are usually heterogeneous catalysts. The extremely small size of the particles maximizes surface area exposed to the reactant, allowing more reactions to occur. However, thermal stability of these nanomaterials is limited by their critical sizes; the smaller the crystallite size, the lower the thermal stability. In this chapter the characterization of metal oxides such as CeO_2, TiO_2, and ZnO and some of their applications as catalysts for methane combustion and photocatalysis is described. The effects of mixed oxides, and mixed phases were investigated.

Keywords: catalytic combustion, photocatalysis, cerium oxide, titanium oxide, zinc oxide.

7.1 Introduction

Catalysts are typical nanomaterials, perhaps the first nanomaterials in wide applications. Catalysis is a nanoscale phenomenon that has been the subject of research and development for many years, but only recently has it become a nanoscale science of materials and chemistry involving more investigations on the molecular level.

Nanomaterial-based catalysts are usually heterogeneous catalysts. The extremely small size of the particles maximizes surface area exposed to the reactant, allowing more reactions to occur. However, thermal stability of these nanomaterials is limited by their critical sizes; the smaller the crystallite size, the lower the thermal stability.

Here, the characterization of metal oxides such as CeO_2, TiO_2, and ZnO and some of their applications as catalysts for methane combustion and photocatalysis is described. The effects of mixed oxides and mixed phases were investigated.

7.2 Catalytic Combustion

Ceria has been included in automotive emissions-control catalysts for many years and ceria-supported metals are finding new applications in hydrocarbon-reforming and in hydrocarbonoxidation catalysis [1].

In these applications, the ability of cerium to change its valence between Ce^{+3} and Ce^{+4} is decisive; however, the mechanisms by which ceria promotes reactions are not fully comprehended [2]. The prominent role of ceria has been recognized in three-way catalysis, catalytic wet oxidation, water-gas-shift reaction, oxidation/combustion catalysis and solid oxide fuel cells [3].

Ceria can be employed as an oxide carrier or a mixed oxide carrier with a transition metal oxide providing unique catalytic properties. Ceria is also believed to help in preserving the catalyst surface area, pore size distribution and catalytic activity. Several CeO_2-based systems such as CeO_2-ZrO_2, CeO_2-Al_2O_3, $CuO/CeO_2/Al_2O_3$, CeO_2-SiO_2, Pd/CeO_2 and Au/CeO_2 have been examined for their catalytic properties. Recently, efforts have also been made to synthesize nanostructured ceria particles with better physicochemical properties for diverse applications.

7.2.1 Structural Features of CeO_2

The structural properties of CeO_2 have been investigated by several authors providing valuable information on redox properties and oxygen mobility in the ceria lattice [4-6].

Ceria is a pale yellow color solid known to crystallize in fluorite structure (CaF_2) with a space group of Fm3m [7]. The unit cell of ceria is shown in Figure 7.1. In the face centered cubic (FCC) structure of ceria, Ce^{4+} ions form a cubic close packed arrangement and all the tetrahedral sites are occupied by the oxide ions whereas the octahedral sites remain vacant.

The fluorite structure of ceria is retained up to 900 K under reducing atmosphere. However, the lattice parameter is found to increase with reduction temperature, indicating an expansion in the FCC lattice [4]. The increase in the lattice parameter is attributed to the reduction of Ce^{4+} ions to Ce^{3+}. The radius of Ce^{3+} is larger than the radius of Ce^{4+} resulting in the lattice expansion. The ability of the cerium ion to switch between the Ce^{4+} and Ce^{3+} oxidation states depending on the ambient oxygen partial pressure is represented as:

$$CeO_2 \Leftrightarrow CeO_{2-x} + \tfrac{x}{2} O_2 \tag{7.1}$$

The amount of oxygen released in this reaction and the oxygen consumed in the reverse reaction is generally referred to as the oxygen storage capacity (OSC) of ceria material.

Under reducing atmosphere, ceria is known to form nonstoichiometric oxides of composition CeO_{2-x} where $0<x<0.5$. The oxidation of CeO_{2-x} occurs at room temperature, while the reduction of CeO_2 starts at 473K. Pure CeO_2 deactivates its OSC usually at 1123K due to its sintering [8].

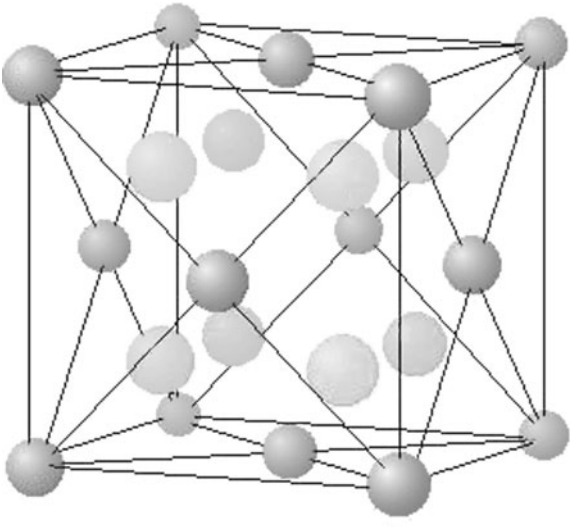

Fig. 7.1. Fluorite structure of CeO_2.

High OSC is believed to be dependent on a high surface area and the phase formed during synthesis. Ceria materials with high OSC are also obtained by cation doping, which produces oxygen vacancies [9].

Ceria in Three Way Catalyst (TWC)

The main application of the OSC of ceria-based materials is in exhaust catalysis, extensively reviewed in the literature [10-15]. The three-way catalysts are designed to convert automobile exhaust pollutants such as uncombusted hydrocarbons (HC), carbon monoxide (CO) and nitrogen oxides (NOx), to environmentally acceptable products such as carbon dioxide, water and nitrogen.

The TWC formulation usually contains metals (Pt, Rh, and Pd) dispersed on the surface of alumina. High surface area γ-alumina is used as support because of its higher thermal stability under hydrothermal conditions. Ceria and ceria-based mixed oxides are used as oxygen storage promoters in TWC. An optimum performance of the TWC is possible if the stoichiometric air–fuel ratio (A/F) is maintained at about 14.6 [16].

If the air–fuel ratio is close to the stoichiometric value of 14.6, the catalyst converts all the pollutants to CO_2, H_2O and N_2 gases with high efficiency. Under fuel lean periods the conversion of NO is affected whereas under fuel-rich conditions the oxidation of CO and hydrocarbons remains incomplete. The role of ceria and ceria-based materials in TWC is to widen the A/F window and help maintaining the conversion efficiency of the catalyst.

Application of CeO_2 Nanostructured Fibers as Catalyst

Due to more restrictive environmental regulations, nowadays the majority of automobiles with internal combustion engines have a system that controls the emission of exhaust gases: carbon monoxide (CO), hydrocarbon compounds (CxHy) and nitrogen oxides (NOx), called a catalytic converter.

The catalytic converter was invented by Eugene Houdry around 1950, when the results of early studies of smog in Los Angeles were published [17]. Houdry founded a company, Oxy-Catalyst, to develop catalytic converters for gasoline engines [18]. The catalytic converter was further developed by John J. Mooney and Carl D. Keith at the Engelhard Corporation, bought by BASF in 2006, creating the first three-way catalytic converter in 1979/80 [19].

A typical catalytic converter is based on CeO_2 doped with noble metals such as Pt and Pd. The efficiency of this converter depends on the activity of the catalyst. There are several industrial applications of nanostructured CeO_2 catalysts and almost every car manufacturer develops its own CeO_2 catalytic system [20-23].

In this chapter the development of catalysis tests, using nanostructured cerium oxide doped with copper fibers, is discussed. The fibers were obtained using the electrospinning process. To summarize, the electrospinning process uses a high power supply to generate an electrical field on which a polymer solution containing ions is accelerated and elongated, forming fibers of micro to nanoscale diameters. More details on the electrospinning process can be found in the literature [24-26].

The structure of the fibers produced using this technique can be seen in Figure 7.2a and b.

(a)

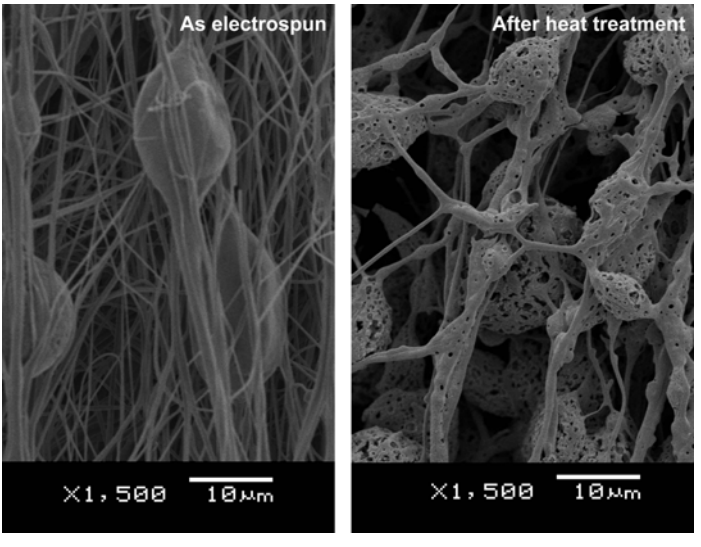

(b)

Fig. 7.2. (a) Photography of the CeO_2 fiber-mat obtained using the electrospinning process. (b) SEM image of the fiber mat showing the microstructure of the fibers.

The average size of the crystallites of the electrospun CeO_2 fibers is 25nm. Figure 7.3 presents a TEM showing a nanostructured fiber. One can notice that a single fiber contains several crystallites in nanoscale.

This fibrous material was used as a catalyst in the combustion of methane in air under different temperatures. The apparatus built to analyze the catalytic activity of the fibers consists of a vertical tubular furnace, a quartz tube reactor, a set of methane and air flow controllers, and a thermocouple for measuring the temperature of the reaction. The air and methane flow was kept constant at 0.9 L/min and 0.1 L/min, respectively. The amount of sample used was approximately 0.2 g.

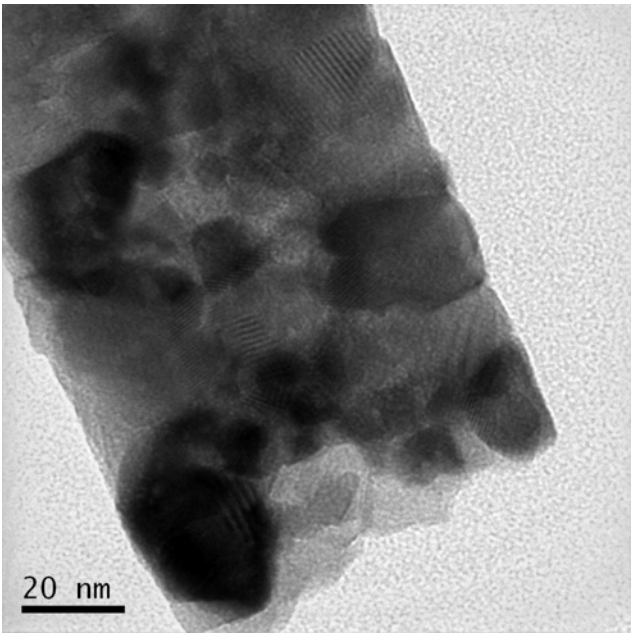

Fig. 7.3. TEM image of the nanostructured CeO_2 fibers obtained by electrospinning.

In a typical catalytic combustion test the sample is loaded into the quartz reactor, and set into the furnace. The gas mixture inlet is connected to the quartz reactor. The temperature of the furnace is set to reach 600°C in 60 minutes with a dwell time at 600°C of 5 minutes. A gas analyzer ECOLINE 4000 was used to analyze the quantities of O_2, CO, CO_2, NO, NOx and CxHy, consumed or generated during the reaction time.

The results of the catalysis tests using cerium oxide doped with 0.5, 1 and 2,5% are presented in Figure 7.4 in terms of the conversion of methane. The ignition temperature and the total methane conversion using the different amounts of copper are presented in Table 7.1.

Table 7.1. Composition of the catalyst ignition temperature and methane conversion.

Catalyst	**Ignition Temperature (°C)**	**Methane Conversion (%)**
CeO_2	594	85.4
CeO_2 + 0.5% Cu	559	100.0
CeO_2 + 1.0% Cu	576	91.0
CeO_2 + 2.5% Cu	593	71.2

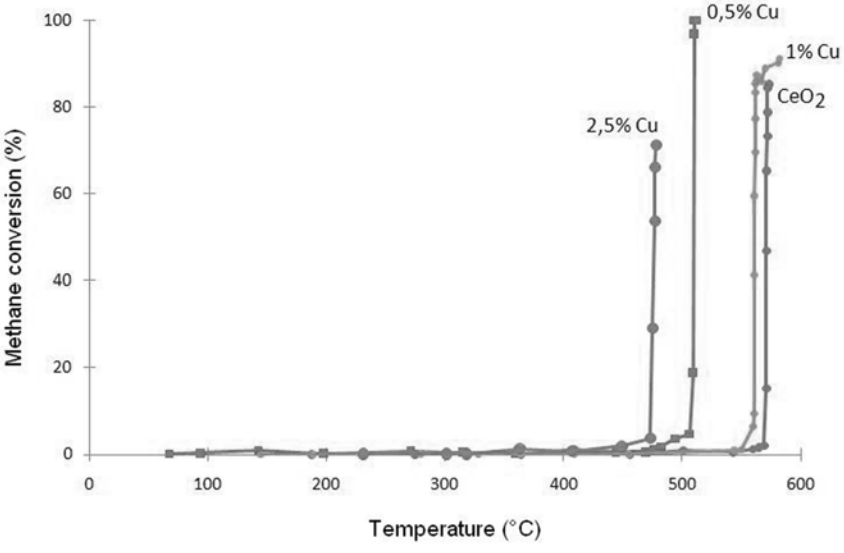

Fig. 7.4. Conversion of methane during the catalysis tests using cerium oxide doped with 0.5, 1 and 2,5%.

One can observe that the addition of more than 1% of copper has no beneficial effects over the reaction conversion. The presence of a metal such as copper over cerium oxide promotes the catalytic effect of the combustion reaction, but this effect is apparently limited to 1% of copper.

7.3 Photocatalysis

7.3.1 Introduction

Photocatalysis is a process where a chemical reaction is accelerated in the presence of a catalyst that is only active in the presence of light (ultraviolet or visible light). The oxidation of most hydrocarbons proceeds slowly in the absence of a catalytic active substance. A photocatalyst decreases the activation energy, making photoinduced processes occur.

A photocatalytic system usually consists of a semiconductor particle (photocatalyst) which is in close contact with a liquid or a gaseous reaction medium. When a semiconductor is exposed to UV light for example, redox reaction will occur at the surface of the catalyst generating hydroxyl radicals ($^{\bullet}OH$) and superoxide ions (O^{-2}). These oxidizing agents are able to decompose organic compounds into CO_2 and H_2O [27].

The most common photocatalysis applications are: conversion of water to hydrogen gas by photocatalytic water splitting; self-cleaning glasses, textiles and

surfaces; disinfection of water; oxidation of organic contaminants using magnetic particles that are coated with photocatalyst nanoparticles; conversion of carbon dioxide into gaseous hydrocarbons; as an UV light absorber; sterilization of surgical instruments; among many other applications [28].

7.3.2 Titanium Oxide

Nanocrystalline photocatalytic materials are a potentially lucrative area of nanomaterials development [20]. Industrial utilization of the photocatalytic effect of nanomaterials is already seen in applications such as self-cleaning tiles, windows and textiles, anti-fogging car mirrors, and anti-microbial coatings [29-32]. For the photocatalysis market, nanostructured titanium dioxide (TiO_2) is the most suitable material for industrial use at present and promises innovative products in the future.

The commercial potential of nanoscale TiO_2 coatings is enormous, including applications in medicine, architecture (cultural heritage protective/recuperation purposes, facade paints, indoor, wall paper, tiles, etc.), the automotive and food industries (cleaner technologies, non-fogging glass and mirrors, product safety), the textile and glass industries, and in environmental protection (water and air purification and disinfection) [33-38].

Titanium dioxide nanoparticles (anatase and/or rutile phases) are able to generate excited ions by promoting electrons across theirs band gaps. The electrons and holes react with the surrounding water molecules to produce hydroxyl radicals and protons. These radicals mineralize organic compounds to CO_2 and H_2O. For pure titanium dioxide this effect only occurs under UV illuminating, while Visible light may produce this effect in doped titanium dioxide.

Application of TiO_2 Nanostructured Fibers as Photocatalyst

Commercial nanostructured TiO_2 photocatalysts are made by several different companies around the world. The most studied and published photocatalyst is made by Evonik Industries using the high-temperature flame hydrolysis; it is known as AEROXIDE® TiO_2 P25 [24]. P25 is commonly used as a standard photocatalyst and many researches are developing new materials to achieve its high photocatalysis efficiency.

In this chapter the photocatalysis tests were made with nanostructured titanium dioxide fibers and the results compared with TiO_2 P25. The fibers were obtained using the electrospinning process. To summarize, the electrospinning process uses a high power supply to generate an electrical field on which a polymer solution containing ions is accelerated and elongated, forming fibers of micro to nanoscale diameters. More details on the electrospinning process can be found in the literature [24-26].

The structure of the titanium dioxide fibers produced using this technique can be seen in Figure 7.5a, b and c.

(a)

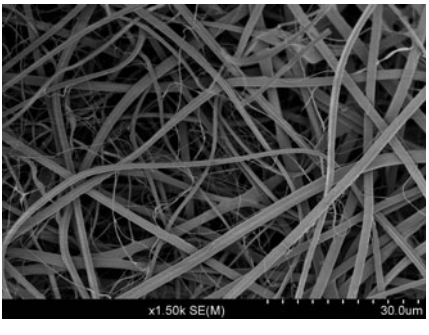

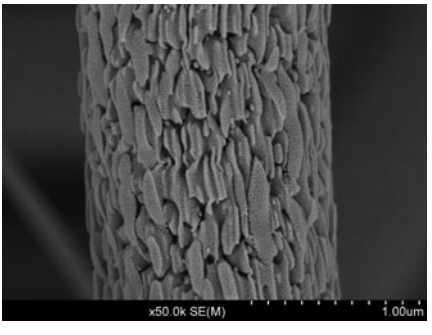

(b) (c)

Fig. 7.5. (a) Photography of the TiO_2 fiber-mat obtained using the electrospinning process. (b) SEM image of the fiber mat showing the microstructure of the fibers. (c) High resolution FESEM image showing details of the microstructure of a single fiber.

The average size of the crystallites of the electrospun TiO_2 fibers is 20nm. Figure 7.6 presents a TEM showing a nanostructured fiber. One can notice that a single fiber contains several crystallites in nanoscale.

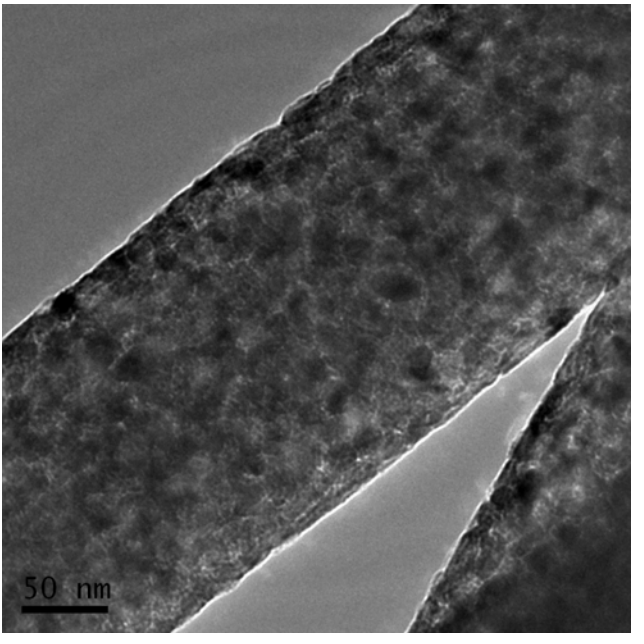

Fig. 7.6. TEM image of the nanostructured TiO_2 fibers obtained by electrospinning.

This fibrous material was used as a model photocatalyst in the decomposition of organic dyes, such as methylene blue (MB) and methyl orange (MO). The apparatus built to analyze the photocatalytic activity of the fibers consists of a Dreschel glass flask of 130mL equipped with a rubber septum to collect samples. This flask is located between two half cylinders, each with a set of 12 Ultra-Violet (black light) or Visible T8 type lamps. The system also contains a magnetic stirrer, an air bubbler and a thermostatic bath to keep the reaction temperature constant at 30°C. More construction details of this equipment can be found in the work of Alves, et al. [39].

A typical photocatalysis experiment consists of mixing 50mg of the catalyst with 125mL of a 20ppm dye solution. This mixture is homogenized with the help of an ultrasound finger for about 15 minutes. After this period a 4 mL sample of this solution is taken and poured into a PMMA spectrophotometer cuvette. The solution is transferred to the Dreschel flask and the air bubbler and the UV or visible lights are turned on. Samples are then taken every 5 minutes to follow the photodecomposition of the dye. After about 60 minutes of irradiation the samples are analyzed using a Uv–vis spectrophotometry.

The results of the photoactivity of the fiber in comparison with P25 are depicted in Figure 7.7 for the decomposition of methylene blue under UV illumination.

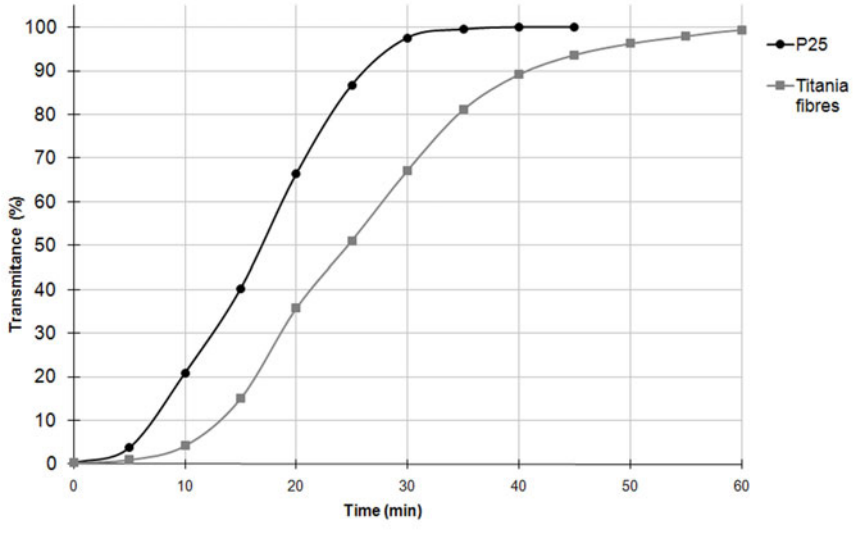

Fig. 7.7. Decomposition of methylene blue under UV light using TiO_2 nanostructured fibers and P25.

It is well known that the pH of the medium strongly influences the photocatalytic reactions. An analysis of the effect of the pH on the photoactivity of the nanostructured fibers was made using methyl orange as a dye model. Methyl orange was the selected model dye because of its high stability in the entire pH range. The results of these experiments are depicted in Figure 7.8.

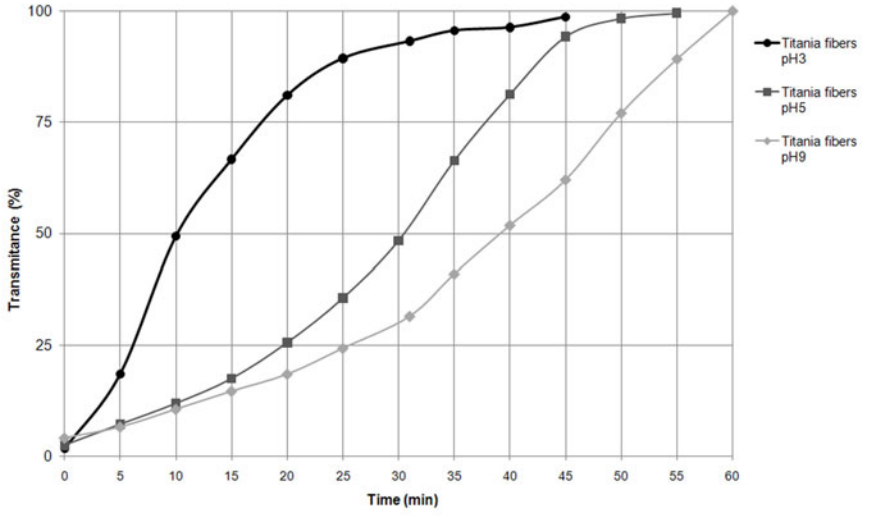

(a)

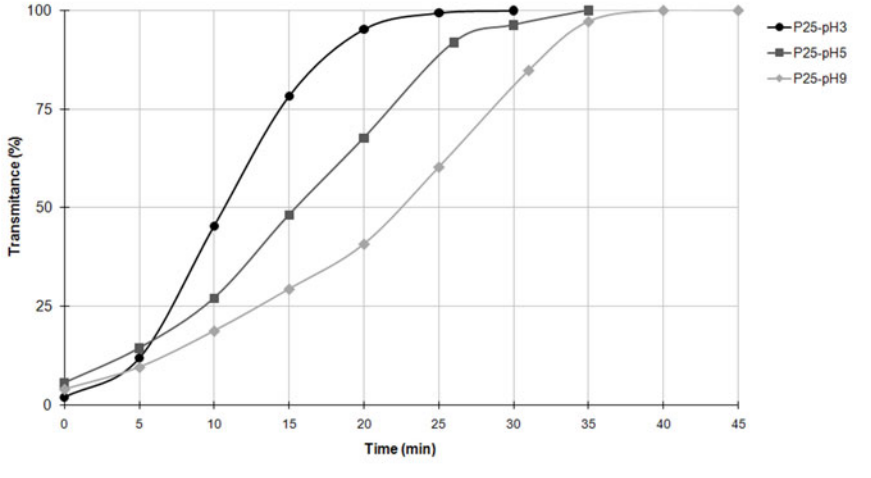

(b)

Fig. 7.8. Decomposition of methyl orange under UV light using (a) TiO_2 nanostructured fibers and (b) P25, under different pH condition.

Doping TiO_2 with other metals can promote the photocatalytic effect in visible light. During the preparation of the TiO_2 nanostructured fibers using electrospinning, different amounts of tin were added to study the contribution of this metal in the UV and Visible photoactivity of TiO_2. The results of these experiments under

UV light are depicted in Figure 7.9 and the results of the experiments under Visible light are depicted in Figure 7.10.

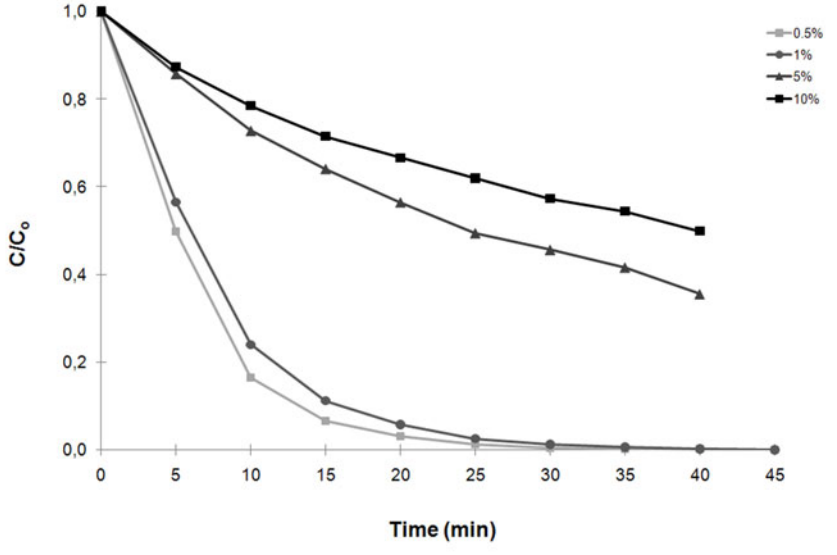

Fig. 7.9. Photodecomposition of methyl orange under UV light using TiO_2 nanostructured fibers doped with tin.

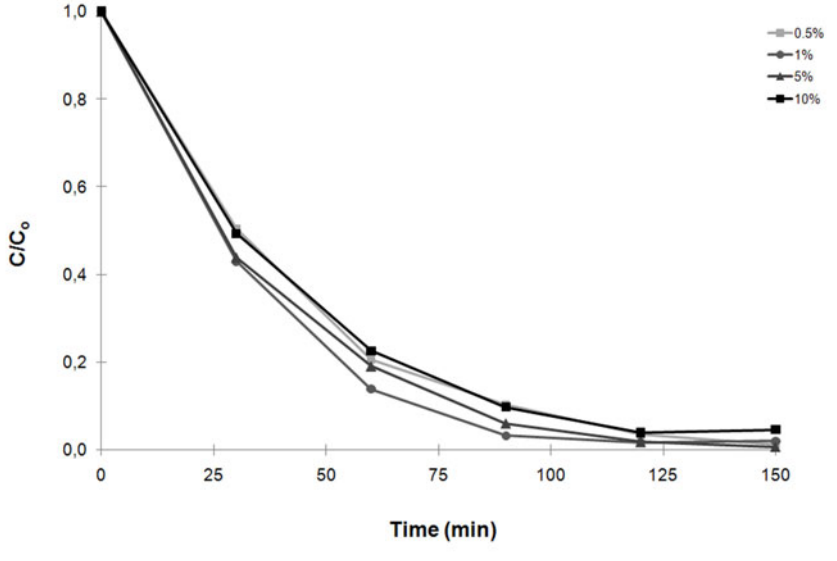

Fig. 7.10. Photodecomposition of methyl orange under Visible light using TiO_2 nanostructured fibers doped with tin.

Nanostructured fibers of TiO_2, with and without tin, obtained using the electrospinning technology was highly active in UV and Visible light.

7.3.3 Zinc Oxide

Zinc oxide is an inorganic compound with ZnO as chemical formulation. In high purity levels it is a white powdery substance, which is nearly insoluble in both water and alcohol, but soluble in most of the acids including hydrochloric acid. Due to its variety of interactive properties in distinct kinds of combined systems or compositions, zinc oxide has an extensive gamma of profitable uses in a wide range of industrial applications in different technological fields. Some well known and significant industrial applications of this versatile material are described below:

• Rubber Industry: The chemical reactivity of zinc oxide contributes to activate the organic accelerator, to speed up rubber cure rate. It is also useful to protect latex plantation because it reacts with the enzyme responsible for its decomposition. Due to its dielectric properties, zinc oxide improves the resistance to corona effects since its dielectric strength maintains a series of physical properties of rubber compounds at high operating temperatures and, similarly, because it retards devulcanization of many types of rubber compositions operating at elevated temperatures. Through its high brightness, refractive index, and optimum particle size, zinc oxide provides a high degree of whiteness and tinting strength for such rubber products as tire side walls, sheeting and surgical gloves.

• Ceramic Industry: Some of its newer applications are as electronic glass, low-melting glass for metal-to-glass seals, thermistors for use as lighting arresters and devitrified glasses of low thermal expansion. Zinc oxide plays an important role in semiconductor ceramic elements for operation at elevated temperatures or high voltages. Thermoelements such as varistors are composed of zinc oxide semiconductors modified or doped by other elements and can be produced to cover a broad range of thermal and electrical needs.

• Pharmaceutical and cosmetic Industries: Zinc oxide is mainly used in zinc soap, ointment, dental inlays, food powders, etc. Its optical and biochemical properties impart special features to a variety of cosmetic preparations for hair and skin care. In powders and creams it protects the skin by absorbing the ultraviolet sunlight rays and in burn ointments it aids healing.

• Plastics Industry: In plastics manufacturing, zinc oxide offers a large range of advantages such as mechanical and thermal resistance and it increases the lifetime of some polymer products by stabilizing them against aging and UV radiation as well.

• Paint Industry: Zinc oxide in organic coatings provides a broad spectrum of optical, chemical, biochemical and physical properties. Over the past century the paint industry, in its constant development of improved products, has utilized various aspects of those properties to a high degree.

• Adhesives Industry: Zinc oxide has long been a major constituent of surgical and industrial tapes based on natural or synthetic rubber as it is outstanding in retention of tack during shelf aging.

• Foods and Food-Packaging Industries: Zinc oxide and its derivatives contribute specially as fungistatic element and because of its chemical properties to the processing and packaging of various animal and vegetable products. It has long been incorporated into the varnish linings of the metal containers to prevent formation of black sulfides which discolor the food.

Other zinc oxide applications include its use in industrial lubrificants composition, in the photocopying process, in cigarette filters, for sulfur removal in fluids, in Portland cement composition and as a component of batteries, fuel cells and photocells.

This oxide occurs in the Earth's crust as a mineral, known as zincite and can be found in a few deposits all over the world. However, industrial production of zinc oxide is basically obtained by three general methods [40]:

• The French process: Also known as the indirect process, this technique starts by heating pure metallic zinc in an appropriate crucible until the boiling point (temperatures above 907 °C). The zinc vapor obtained naturally reacts with the oxygen in the air, resulting in a white, zinc oxide powder due to an oxidation reaction. The particles are transported into a cooling duct and collected in an adequate particle trap system. This indirect method was popularized by LeClaire (France) in 1844 and therefore is commonly known as the French process. Its product normally consists of agglomerated zinc oxide particles with an average size of 0.1 to a few micrometers. By weight, most of the world's zinc oxide is manufactured via the French process.

• The direct (American) process: In the direct process, the starting materials are various contaminated zinc composites, such as zinc ores or smelter by-products. It is reduced by heating with a carbon additive (e.g. anthracite) to produce zinc vapor. The generation of carbon monoxide reduces the oxidic zinc and the zinc is expelled as vapor. The zinc is reoxidized when it comes into contact with lower temperature air, forming zinc oxide particulate. The combination of the reduction reaction and the zinc vapor pressure combine to purify the zinc which is then oxidized as in the indirect process. Because of the lower purity of the source material, the final product is of lower quality in the direct process as compared to the indirect one.

• Wet chemical processes: These routes usually start with purified zinc solutions from which zinc carbonate or zinc hydroxide are precipitated. Before the final product is obtained, some stages are required, such as, filtration, washing, drying and calcination (mild temperatures ~ 800°C). For example, this zinc oxide is produced as a co-product with sodium hydrosulfite, a bleaching agent used primarily in the Paper Industry. Sulfur is present as zinc sulfide and other sulfur containing compounds, with total sulfur content reaching up to 2% and producing a lemon-yellow colored powder. Grades which are manufactured from precipitated zinc hydroxide or basic zinc carbonate intermediates are often termed as active zinc oxide. Mild heat treatment decomposes the materials into zinc oxide. This oxide is relatively reactive, due to its very high surface area which can be above 50 m^2/g. Such products are useful in catalysts and latex rubber applications.

Other controlled thermal treatments make possible the generation of suitable products for different markets. There is a very wide range of specifications for different end uses and geographical locations, how these are met depends on the practices of the individual zinc oxide manufacturer.

Zinc oxide production occupies an important place in the structure of the global zinc market. The annual global consumption of zinc is 10.5-11 million tons, and about 8% of it is used in the zinc oxide production. The largest consumption sector of this product is the Rubber Industry for the manufacture of tires and mechanical rubber goods [41].

Zinc oxide is a semiconductor with a large exciton binding energy (60 meV), direct band-gap (E_g = 3.37 eV) exhibiting near UV emission, transparent conductivity and piezoelectricity. Moreover, it is biosafe and biocompatible, and may be used for biomedical applications without coating.

Intensive research has been focused on the fabrication of zinc oxide nanostructures and on correlating their morphologies with their size-related optical and electrical properties [42-46]. Various kinds of zinc oxide nanostructures have been realized, such as nanobelts, nanodots, nanorods, nanowires, nanotubes, nanobridges, nanonails, nanowalls, nanohelixes and seamless nanorings among other varieties [47-49].

Strict parameter controls of conventional zinc oxide processes as well as some adaptations in the ordinary techniques are the key in the development of zinc oxide nanostructured powders, which will be referred to from this point as “nano-ZnO”. Two different techniques are being developed by the authors and will be further detailed in this chapter.

The European Commission has listed nano-ZnO as one of the major nanomaterials to be intensely commercialized between 2006 and 2014. Nano-ZnO has attracted lots of basic research funding due to its highly versatile and promising applications in biotechnology (antibacterial, antifungal and antifouling), UV protection (sunscreens, paints, polymer nanocomposites and rubber), optoelectronics (LEDs, hydrogen fuel, toner, sensors), among other exposed applications [50].

The global production of zinc oxide equals over 1 million tons of zinc oxide per year [51], less than 1% of this, however, is nano-ZnO. Currently, the major production of nano-ZnO is mainly to supply the Sunscreen Industry where nano ZnO (together with TiO2) serves as the UV absorber. Around 30% of sunscreen lotion uses nano ZnO particles [52] as the photocatalysts that protects the human skin from dangerous UV rays of sunlight.

Due to the remarkable photochemical reactivity of nano-ZnO, it can match the reactivity of micrometric ZnO with far smaller amounts of nano-ZnO, and this approach, in turn, can greatly reduce the release of toxic zinc metal into the environment.

Most of the work on nano-ZnO is still at the basic research stage [50]. It is expected that by 2015, ZnO nanomaterials will be mass produced in a much larger tonnage for various applications in automotive catalysis, sunscreens, antibacterial products, rubber vulcanization, fungicides, pigments, nano-textiles, high-performance coatings, water treatment, dental fillings, hydrogen fuel systems,

chemical sensors, pollutant filters, toner photoconductor, and optoelectronics [50, 53-54]. In any case, it is possible to find several industries spread around the world that are producing different kinds of nanostructurated zinc oxides on a large scale [55-61].

Photocatalytic Activity Applications of Nanostructured Zinc Oxide

Semiconductor materials such as zinc oxide show a vast number of interesting properties, which are maximized when these belong to the nanostructured materials as has already been discussed previously. However, one of the emerging and intensively explored properties of this nanostructured oxide is its photocatalytic activity mainly for the treatment of environmental pollution.

The Environmental Protection Agency (USA) has listed several volatile organic compounds as contaminants in ground water. The list includes several chlorinated aromatic and aliphatic compounds such as 4-chlorophenol, pentachlorophenol, chlorobenzene, dichlorobenzene, carbon tetrachloride, chloroform, dichloroethylene, trichloroethylene and dichloromethane, and other common organic solvents such as phenols, toluene, benzene and xylenes [62].

Established waste water treatments such as activated carbon adsorption, membrane filtration, ion exchange on synthetic adsorbent resins, chemical coagulation, etc., also generate wastes during the water treatment process, which requires additional steps and consequently more investment. In recent years, the heterogeneous photocatalytic oxidation (HPO) process employing ZnO and UV light has emerged as a promising new route for the degradation of persistent organic pollutants, and produces more biologically degradable and less toxic substances [63-64].

The photocatalytic phenomena of zinc oxide occur due to the presence of a large number of defects in the crystalline structure such as oxygen vacancies, interstitial zinc atom from the donor states, zinc vacancies and intestinal oxygen atoms from the acceptor states. The electronic condition created in this structural arrangement produces a band-gap, an intrinsic characteristic of semiconductor materials, by the existence of a forbidden gap between the valence and the conduction band. The photocatalytic activity of zinc oxide occurs only when photons with energies greater than the band-gap energy can result in the excitation of valence band electrons, which can then promote a reaction. The absorption of photons with lower energy than the band-gap energy or longer wavelengths, usually causes energy dissipation in the form of heat. The illumination of the photocatalytic surface with sufficient energy leads to the formation of a positive hole in the valence band and an electron in the conduction band [65]. After the light excitation the pair electron-hole created could have an electronic recombination releasing heat or could be involved in electronic transfer with other species and interact directly or through some photosensitizers with organic substrates. The positive hole oxidizes either pollutant directly or water to produce hydroxyl radicals (•OH), whereas the electron in the conduction band reduces the oxygen adsorbed on the catalyst [66]. Based on this principle zinc oxide and more recently nano-ZnO have received attention in research on the degradation of different organic specimens that are environmental pollutant.

An important feature in the environmental photocatalysis is the selection of semiconductor materials such as ZnO and TiO_2, which are close to being two of the ideal photocatalysts in several research proposals. These oxides are relatively inexpensive, and they provide photogenerated holes with high oxidizing power due to their wide band gap energy [67]. Since ZnO has almost the same band-gap energy as TiO_2, its photocatalytic capacity is anticipated to be similar to that of TiO_2. However, in the case of ZnO, photocorrosion frequently occurs with the illumination of UV light, and this phenomenon is considered one of the main reasons for the decrease of ZnO photocatalytic activity in aqueous solutions [68,69]. However, some studies have confirmed that ZnO exhibits a better efficiency than TiO_2 in photocatalytic degradation of some dyes, even in aqueous solution [70,71]. ZnO has sometimes been reported to be more efficient than TiO_2. Nevertheless, the biggest advantage of ZnO is that it absorbs over a larger fraction of the solar spectrum than TiO_2 [72]. For this reason, ZnO is quite suitable photocatalyst for photocatalytic removal in the presence of sunlight [73].

As was previously mentioned in this chapter, two researches that are being developed by the authors focused on the production of nano-ZnO powders will be described. This nanostructured material is being produced, on the one hand, by a suitable adaptation of the extensively used industrial technique (French process) and, on the other hand, based on a flame synthesis process.

The first nano-ZnO process mentioned is based on the thermal evaporation of pure metallic zinc in an oxidative atmosphere and is in development as an industrial prototype. It consists basically of a horizontal tube furnace with strict control of parameters such as temperature of the reactional environment, gas flow and the position of the injection points of the gases. The apparatus that was newly developed is passing through a patent request process. The methodology employed appears to be an interesting alternative for producing nano-ZnO on a large scale without any residual pollutants. Depending on the procedural conditions, the nano-ZnO produced can be either shaped as nanowires or nanotetrapods, with a white, agglomerated powder aspect.

The second technique developed for obtaining nano-ZnO consists of a flame synthesis. This flame-based equipment was also completely assembled in the laboratory. This method, basically, consists of forming a spray from a liquid combustible solution as the precursor, which is then burnt at the high temperatures of the flame, producing the nano-ZnO product, which is later collected in a powder collector system [74]. The nano-ZnO produced is composed of espherical primary nanoparticles that remain in an aggregated state. Flame-based techniques are a continuous and well-established method and are considered cost-effective processes that have the potential for large scale nanoparticles production [75,76].

The wide range of morphologies of nano-ZnO are well illustrated in the literature as well as the considerable amount of processes and applications that are being developed. It is also clear that each nanostructure created proves to have great effects on their widely varying properties and corresponding potential applications [77-80].

An interesting approach at this point is to compare the photocatalytic activity of both nano-ZnO materials synthesized by the authors through the mentionated

procedural techniques and have an evident distinct morphology. Figure 7.11 shows micrographies produced by scanning electron and transmission electron microscopic techniques of both nano-ZnO powders. The thermal evaporation-based nano-ZnO (ZnO TEb) reveals a structural shape of tetrapods with an acicular edge diameter of 30–50 nm and a core diameter of a few micrometes. The flame synthesis-based nano-ZnO (ZnO-FSb) shows the primary particles with a spherical shape with 20–40 nm of diameter. The specific surface area of the nano-ZnO powders, measured by Brunauer–Emmett–Telle (BET) N_2 sorption technique, results in significantly different values corresponding to 8.35m²/g for ZnO-TEb and 17.34 m²/g for the ZnO-FSb. The discrepancy of the measurements can be attributed to the powder agglomeration that the nanotetrapod shaped ZnO acquired after being processed as well as to some metallic zinc that could remain after processing, which is being investigated.

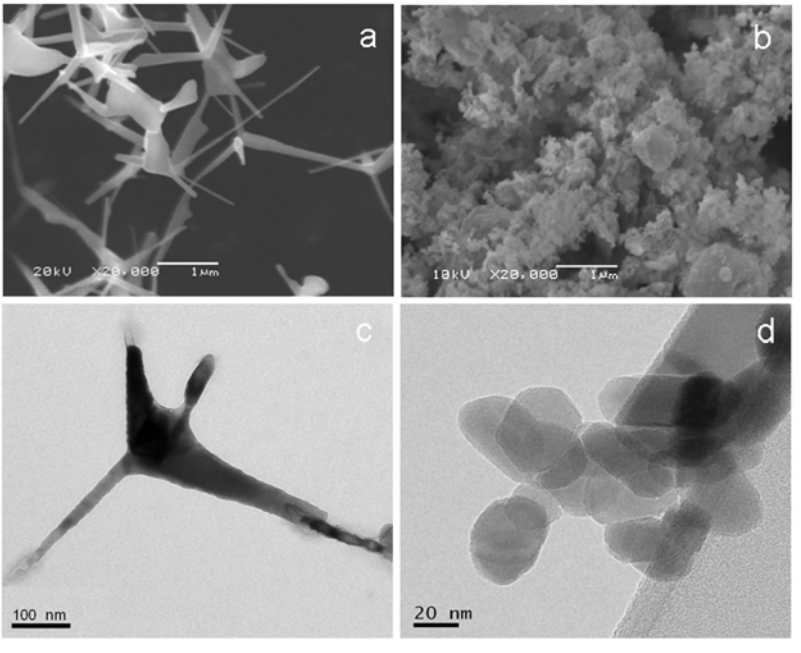

Fig. 7.11. Scanning electron migrographies of nano-ZnO obtained via the French process (a) and the Flame process (b). Transmission electron micrographies of nano ZnO obtained via the French process (c) and Flame process (d).

The photocatalyitic activity of the nano-ZnO was measured by the evaluation of a standard solution of methyl orange (MO) in a photochemical reactor using the same methodology as described in the work of Trommer R. M. et al [74]. Figure 7.12 shows the photocatalytic degradation of MO by the nano-ZnO obtained. One can observe that in a period of 20 min the ZnO-TEb reaches almost 80% of MO degradation while the ZnO-FSb achieves 10% of degradation.

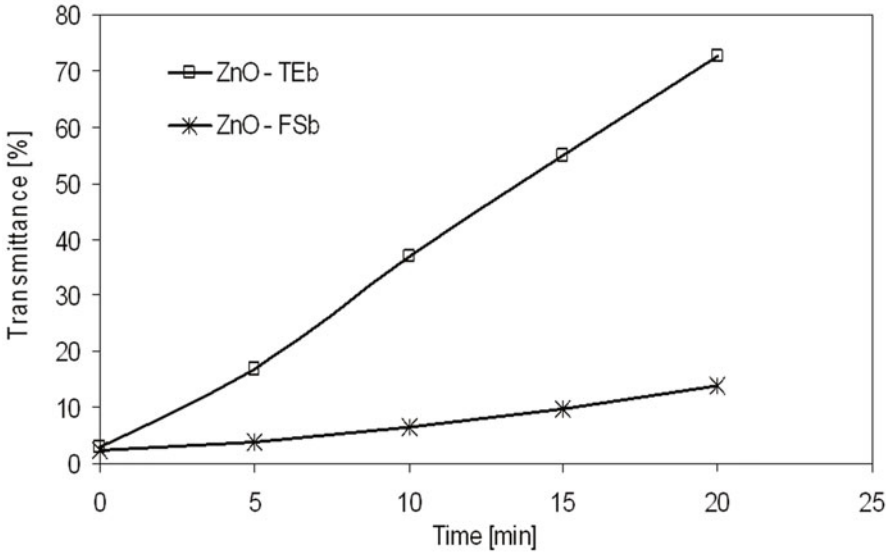

Fig. 7.12. Photocatalytic activity of nano-ZnO with different morphology described by a Transmittance versus time in the degradation of methyl orange dye.

The different behavior of the nano ZnO materials can be attributed to the morphology of the nanoparticles and not to the specific surface area. Some research discusses the improvement of the photocatalytic activity of particulate systems through the decrease of particle size at nanometric scale [81-83]. Decreasing the average particle size increases the specific surface area and consequently increases the number of active surface sites where photogenerated charge carriers are able to react with adsorbed molecules to form free radicals. Decreasing the particle size of a photocatalysts, though, also increases the rate of surface charge recombination [84]. As a consequence the activity of photocatalyst nanoparticles does not increase with decreasing particle size inferring that some alternatives to inhibiting charge carrier recombination are required to verify this behavior [85].

An argument proposed by Y. Wang et al [86] indicated that the differences in the photocatalytic activity of distinct nanostructures of zinc oxide could be associated with the number of oxygen vacancy sites present. These vacancies act as active center and are the main reason for causing the difference in photocatalytic activities for varied morphologic nano-ZnO.

7.4 Concluding Remarks

Summarizing: it is strictly necessary to understand the physiochemical principles involved and correlated with the photocatalytic behavior of species such as TiO_2 and ZnO. Comprehending the behavior of these materials in different environments such as water or air, as well as the radiation used to stimulate the

photocatalytic activity and correlating these systems with the morphology and particle size of the material to be used, are fundamental to develop a guide for the treatment of organic pollutants and consequently to find other uses for such potential photocalatysts semiconductor nanomaterials.

References

[1] Deraz NM (2009) Influence of ceria on physicochemical, surface and catalytic properties of alumina supported manganese catalysts. Colloids and Surfaces A: Physicochemical and Engineering Aspects 335:8-15
[2] Gorte RJ (2010) Ceria in Catalysis: From Automotive Applications to the Water–Gas Shift Reaction. Reactors, Kinetics, And Catalysis 56:1126-1135
[3] Petar D, Levec J, Pintar A (2008) Effect of structural and acidity/basicity changes of $CuO–CeO_2$ catalysts on their activity for water–gas shift reaction. Catalysis Today 138:222–227
[4] Perrichon V, Laachir A, Bergeret G, Frety R, Tournayan L (1994) Reduction of cerias with different textures by hydrogen and their reoxidation by oxygen. J Chem Soc Faraday Trans 90:773-781
[5] Ricken M, Nolting J, Riess I (1984) Specific heat and phase diagram of nonstoichiometric ceria ($CeO_{2–x}$). J Solid State Chem 54: 89-99
[6] Korner R, Ricken M, Nolting J, Riess I (1989) Phase transformations in reduced ceria: Determination by thermal expansion measurements. J Solid State Chem 78:136-147
[7] Shi C, Yang L, Cai J (2007) Cerium promoted Pd/HZSM-5 catalyst for methane combustion. Fuel 86:106-112
[8] Trovarelli A, Leitenburg C, Boaro M, Dolcetti G (1999) The utilization of ceria in industrial catalysis. Catalysis Today 50:353-367
[9] Trovarelli A (2002) Structural properties and nonstoichiometric behavior of CeO_2. In: Catalysis by Ceria and Related Materials, Imperial College Press
[10] Ghandi HS, Piken AG, Shelef M, Deloch RG (1976) Automotive Engineering Congress and Exposition, Detroit, MI. SAE Paper 760201.
[11] Su EC, Montreuil CN, Rothschild WG (1985) Oxygen storage capacity of monolith three-way catalysts. Appl Catal 17:75-86
[12] Su EC, Rothschild WG (1986) Dynamic behavior of three-way catalysts. J Catal 99:506-510
[13] Engler B, Koberstein E, Schubert P (1989) Automotive exhaust gas catalysts: Surface structure and activity. Appl Catal 48:71-92
[14] Kacimi S, Barbier J Jr, Taha R, Duprez D (1993) Oxygen storage capacity of promoted Rh/CeC_2 catalysts. Exceptional behavior of $RhCu/CeO_2$. Catal Lett 22:343-350
[15] Duprez D, Descorme C, Birchem T, Rohart E (2001) Oxygen Storage and Mobility on Model Three-Way Catalysts. Topics in Catalysis 16-17: 49-56
[16] Rao R, Mishra BG (2003) Structural, redox and catalytic chemistry of ceria based materials. Bulletin of the Catalysis Society of India 2:122-134
[17] The Southland's War on Smog: Fifty Years of Progress Toward Clean Air (1997) http://www.aqmd.gov/news1/Archives/History/marchcov.html. Acessed 20 July 2010.

[18] Houdry EJ, Ardmore P (1952) Catalytic structure and composition. US patent 2742437.
[19] Christian Böhme (2007) The Success of the Automotive Catalytic Converter. http://www.catalysts.basf.com. Acessed 20 July 2010.
[20] Ono M, Okumura A (2010) Exhaust gas putifying catalyst and methos for purifying exhaust gas using catalyst. Patent WO 2010/044454.
[21] Satou A, Takeuchi M, Hiraku K et al Exhaust gas purification catalyst. Patent WO 2010/001215 A2.
[22] Miura M Exhaust gas purifying catalyst and process for producing it. Patent WO 2007/007889 A1.
[23] Kikuchi H, Nakamura M, Wakamatsu H et al Exhaust gas purification catalyst and method for production thereof. Patent WO 2006/054404 A1.
[24] Blake DM, Maness PC, Huang Z, Wolfrum EJ, Huang J (1999) Application of the Photocatalytic Chemistry of Titanium Dioxide to Disinfection and the Killing of Cancer Cells. Separation and Purification Methods 28:1-50
[25] Doshi J, Reneker DH (1995) Electrospinning process and applications of electrospun fibers. Journal of Electrostatics 35:151-160
[26] Shin YM, Hohman MM, Brenner MP, Rutledge GC (2001) Experimental characterization of electrospinning: the electrically forced jet and instabilities. Polymer 42:09955-09967
[27] Hashimoto K, Irie H, Fujishima A (2005) TiO_2 Photocatalysis: A Historical Overview and Future Prospects. Japanese Journal of Applied Physics 44: 8269–8285
[28] Photocatalysis: An Analysis of Its Applications and Market Potential (1998) EPRI, Palo Alto, CA. TR-111898
[29] Gueneau L, Rondet M, Besson S et al. Substrate with a self-cleaning coating. Patent WO 2003/087002.
[30] Funakoshi K, Nonami T (2007) Photocatalytic treatments on dental mirror surfaces using hydrolysis of titanium alkoxide. Journal of Coatings Technology and Research 4: 327-333
[31] Chung CJ, Lin H, Tsou HK, Shi ZY, He JL (2007) An antimicrobial TiO_2 coating for reducing hospital-acquired infection. Journal of Biomedical Materials Research Part B: Applied Biomaterials 85B(1): 220-224
[32] Veronovski N, Rudolf A, Smole MS, Kreže T, Geršak J (2009) Self-cleaning and handle properties of TiO_2-modified textiles. Fibers and Polymers 10:551-556
[33] Shen G, Chen PC, Ryu K, Zhou C (2009) Devices and chemical sensing applications of metal oxide nanowires. J Mater Chem 19:828-839
[34] Haggfeldt A, Bjorksten U, Lindquist SE (1992) Photoelectrochemical studies of colloidal TiO_2-films: the charge separation process studied by means of action spectra in the UV region. Sol Energy Mater Sol Cells 27:293-304
[35] Hermass JM (1999) Heterogeneous photocatalysis: fundamentals and applications to the removal of various types of aqueous pollutants. Catal Today 53:115-129
[36] Ha HK, Yosimoto M, Koinuma H, Moon B, Ishiwara H (1996) Open air plasma chemical vapor deposition of highly dielectric amorphous TiO_2 films. Appl Phys Lett 68:2965-2967
[37] Bahtat A, Bouderbala M, Bahtat M, Bouazaoui M, Mugnier J, Druetta M (1998) Structural characterisation of Er^{3+} doped sol–gel TiO_2 planar optical waveguides. Thin Solid Films 323:59-62.
[38] Desu SB (1992) Ultra-thin TiO_2 films by a novel method. Mater. Sci. Eng. B 13: 299-303

[39] Alves AK, Berutti FA, Clemens FJ, Graule T, Bergmann CP (2009) Photocatalytic activity of titania fibers obtained by electrospinning. Materials Research Bulletin 44:312-317
[40] Porter F (1991) Zinc Handbook: Properties, Processing, and Use in Design. Marcel Dekker Inc, New York.
[41] International Zinc Association. http://www.zincworld.org. Accessed 02 August 2010
[42] Arnold MS, Avouris P, Pan ZW et al (2003) Field-effect transistors based on single semiconducting oxide nanobelts. J Phys Chem B 107:659-663
[43] Keem K, Kim H, Kim GT et al (2004) Photocurrent in ZnO nanowires grown from Au electrodes. Appl Phys Lett 84: 4376-4379
[44] Lee CJ, Lee TJ, Lyu S C et al (2002) Field emission from well-aligned zinc oxide nanowires grown at low temperature. Appl Phys Lett 81:3648-3650
[45] Huang MH, Mao S, Feick H, Yan HQ et al (2001) Room temperature ultraviolet nanowire nanolasers. Science 292:1897-1899
[46] Park WI, Jun YH, Jung SW et al (2003) Excitonic emissions observed in ZnO single crystal nanorods. Appl Phys Lett 82:964-967
[47] Park JH, Choi HJ, Choi YJ et al (2004) Ultrawide ZnO nanosheets. J Mater Chem 14:35-36
[48] Wang ZL (2004) Nanostructures of zinc oxide. Mater Today 7:26-33
[49] Park JH, Choi HJ, Park JG (2004) Scaffolding and filling process: a new type of 2D crystal growth. J Cryst Growth 263:237-242
[50] European Commission (2006) European survey on success factors, barriers and needs for the industrial uptake of nanomaterials in SMEs. http://www.nanoroad.net/download/sme_survey.pdf. Accessed 02 August 2010.
[51] J Lacson (2000) Inorganic zinc chemicals. Chemical Economics Handbook, electronic release. SRI International, Menlo Park CA, USA.
[52] FDA (2006) Public meeting on nanotechnology materials in FDA regulated products, Dept. of Health and Human Services.
[53] P Harrison (2007) Emerging challenges: nanotechnology and the environment. GEO Year Book. United Nations Environment Programme (UNEP), Phoenix Desing Aid, Denmark
[54] Lux Research (2004) Revenue from nanotechnology-enabled products to equal IT and telecom by 2014. Press release
[55] Inframat® Advanced MaterialsTM LLC. http://www.advancedmaterials.us/30N-0801.htm. Accessed 02 August 2010.
[56] Nanophase Technologies Corporation. http://www.nanophase.com/products/details.aspx?ProductId=7. Accessed 02 August 2010.
[57] Evonik Industries. http://nano.evonik.com. Accessed 02 August 2010.
[58] NaBond Technologies Co. http://www.nabond.com/ZnO_nanopowder.html. Accessed 02 August 2010.
[59] M K Impex Canada . http://www.mknano.com. Acessed 02 August 2010.
[60] Nano-Infinity Nanotech Co., Ltd. http://www.b2bnano.com/nanomaterial.htm. Accessed 02 August 2010.
[61] Nanostructured & Amorphous Materials Inc. http://www.nanoamor.com/inc/sdetail/18824. Accessed 02 August 2010.
[62] Hoffmann MR, Martin ST, Choi W et al (1995) Environmental Applications of Semiconductor Photocatalysis. Chem Rev 95:69-96

[63] Li D, Haneda H, (2003) Morphologies of zinc oxide particles and their effects on photocatalysis. Chemosphere 51:129-137
[64] Dindar B, Icli S (2001) Unusual photoreactivity of zinc oxide irradiated by concentrated sunlight. J Photochem Photobiol A: Chem. 140:263-268.
[65] Ahmed S, MG Rasula, Wayde NM et al (2010) Heterogeneous photocatalytic degradation of phenols in wastewater: A review on current status and developments. Desalination 261:3-18
[66] Parida KM, Parija S (2006) Photocatalytic degradation of phenol under solar radiation using microwave irradiated zinc oxide. Solar Energy 80:1048-1054
[67] Hariharan C (2006) Photocatalytic degradation of organic contaminants in water by ZnO nanoparticles: Revisited. Applied Catal A:General 304:55-61
[68] Dijken V, Janssen AH, Smitsmans MHP et al (1998) Size-Selective Photoetching of Nanocrystalline Semiconductor Particles. Chem Mater 10:3513-3522
[69] Neppolian S, Sakthivel B, Arabindoo M et al (1998) Photocatalytic Degradation of Textile Dye Commonly Used in Cotton Fabrics. Stud Surf Sci Catal 113:329–335
[70] Gouvea CAK, Wypych F, Moraes SG et al (2000) Semiconductor-assisted photocatalytic degradation of reactive dyes in aqueous solution. Chemosphere 40:433-440.
[71] Dindar S, Icli J (2001) Unusual photoreactivity of zinc oxide irradiated by concentrated sunlight. Photochem Photobiol A: Chem 140:263-268
[72] Behnajady MA, Modirshahla N, Hamzavi R (2006) Kinetic study on photocatalytic degra-dation of C.I. Acid Yellow 23 by ZnO photocatalyst. J Hazard Mater B 133:226-232.
[73] Qiu R, Zhang D, Mo Y et al (2008) Photocatalytic activity of polymer modified ZnO under visible light irradiation. J Hazard Mater 156:80-85
[74] Trommer RM, Alves AK, Bergmann CP (2010) Synthesis, characterization and photocata-lytic property of flame sprayed zinc oxide nanoparticles. J Alloys Compounds 491:296-300
[75] Roth P (2007) Particle synthesis in flames. Proc. Comb. Inst. 31:1773-1788
[76] Strobel R, Baiker A, Pratsinis SE (2006) Aerosol flame synthesis of catalysts Adv. Powder Technol 17:457-480
[77] Wang ZL;(2004) Zinc oxide nanostructures: growth, properties and applications. J. Phys Condens Matter 16:829-858
[78] Wang N; Cai Y.; Zhang RQ (2008) Growth of nanowires. Mater Sci and Engineering 60:1-51
[79] Wang ZL (2004) Nanostructures of zinc oxide. Mater Today 7:26-33
[80] Polarz S, Pueyo CL, Krumm M (2010) The molecular path to inorganic materials - zinc oxide and beyond. Inorganica Chimica Acta. in press.
[81] Meulenkamp EA (1998) Synthesis and Growth of ZnO Nanoparticles. J Phys Chem B 102:5566-5572
[82] Dodd A, McKinley A, Saunders M et al (2006) A comparative evaluation of the photocatalytic and optical properties of nanoparticulate ZnO synthesised by mechanochemical processing. J. Nanopart Res 10:243-248
[83] Beydoun D, Amal R, Low G et al (1999) Role of Nanopaiticles in Photocatalysis. J. Nanopart. Res. 1:439-458
[84] Dodd A, McKinley A, Tsuzuki T et al (2009) Tailoring the photocatalytic activity of nanoparticulate zinc oxide by transition metal oxide doping. Mater Chem and Phys 114:382–386

[85] Ricci A, Chrétien M, Maretti L et al (2003) TiO_2 promoted mineralization of organic sunscreen in water suspension and sodium dodecyl sulfate micelles. Photochem Photobiol Sci 2:487–492
[86] Wang Y, Li X, Wang N et al (2008) Controllable synthesis of ZnO nanoflowers and their morphology-dependent photocatalytic activities. Separation and Purification Technology 62:727-732

Abbreviations

A/F - Air-Fuel ratio
BET - Brunauer–Emmett–Telle
FCC - Face Centered Cubic
FESEM – Field Emission Scanning Electron Microscopy
ZnO-FSb - Flame Synthesis based nano-ZnO
HPO - Heterogeneous Photocatalytic Oxidation
MO - Methyl Orange
MB - Methylene Blue
OSC - Oxygen Storage Capacity
PMMA - Polymethylmetacrilate
SEM – Scanning Electron Microscopy
TEM – Transmission Electron Microscopy
ZnO TEb - Thermal Evaporation based nano-ZnO
TWC - Three Way Catalyst ()
UV - Ultraviolet